Journal of CO2 Utilization 58 (2022) 101928

Contents lists available at ScienceDirect

Journal of CO2 Utilization

journal homepage: www.elsevier.com/locate/jcou

# Ex-situ mineral carbonation – A parameter study on carbon mineralisation in an autoclave as part of a large-scale utilisation process

Dario Kremer [a,*], Christian Dertmann [b], Simon Etzold [c], Rainer Telle [c], Bernd Friedrich [b], Hermann Wotruba [a]

[a] Unit of Mineral Processing (AMR), RWTH Aachen University, Lochnerstrasse 4-20, 52064 Aachen, Germany
[b] IME Process Metallurgy and Metal Recycling, RWTH Aachen University, Intzestrasse 3, 52056 Aachen, Germany
[c] Department of Ceramics and Refractory Materials, GHI-Institute of Mineral Engineering, RWTH Aachen University, Mauerstrasse 5, 52064 Aachen, Germany

ARTICLE INFO

*Keywords:*
Carbon mineralisation
Carbon capture and utilisation
Olivine
Carbonation

ABSTRACT

The exothermic carbonation reaction includes the degradation of alkaline earth metal (mainly Mg-, Ca-) oxides, hydroxides or silicates under participation of carbon dioxide under aqueous conditions and the formation of stable carbonates with long-term storage of carbon dioxide. The extent of reaction depends on different influencing factors, which significantly affect the economic and ecological feasibility of this technology. With special regard to the possibilities of upscaling and balancing in the context of life cycle analyses for the carbon capture and usage approach, various material-specific and process-related parameters and also combinations of these have been tested experimentally and evaluated. Hereby, significant differences in the carbonation extent were identified with achieved carbonation degrees from below 5 up to 60%, corresponding to 305 $kg_{CO2}/t_{feed}$. This study is a comprehensive investigation of those material-specific and process-related parameters and their combination and aims to ensure the economic viability of enhanced weathering by increasing the degree of carbonation.

## 1. Introduction

The issue of anthropogenic $CO_2$ emissions is a major challenge nowadays and for the immediate future. To meet the objectives set out in the Paris agreement [1], with the aim of keeping the global average temperature increase below 2 K, preferably below 1.5 K above pre-industrial levels, it is no longer sufficient to reduce the carbon dioxide emissions, but negative emissions must be generated. One possible approach for carbon dioxide reduction is carbon capture and utilisation by mineralisation (CCUM). This method of $CO_2$ sequestration by mineral trapping is a safe method to store carbon permanently in a geological sense [2,3]. Despite worldwide large resources of natural feedstock material being available for $CO_2$ sequestration, representing mainly magnesium and calcium silicates, and the technically feasible process, the costs for large-scale carbonation applications are currently too high. Therefore, the challenges of ex-situ carbonation must be overcome by means of improving the process energy economics, the materials handling and the utilisation of reaction products as substitution material and especially the process conditions to enhance both the carbonation degree and the extent of stored carbon to a maximum [4].

In the last 20 years, research on carbonation and ex-situ mineralisation has advanced considerably. The main focus of most studies has been on the highest degree of carbonation without taking into account the costs, required energy, and emissions of the respective processes. This parameter study presents results gathered within the CO2MIN project, which aims at investigating carbonation as a whole. This project considers the achievable carbonation degree of various mineral resources, including their subsequent separation and usage as substitute materials, which also affects the balancing of the entire process regarding ecological and economical considerations [5]. The present study does not cover the balancing of the entire process, which is shown in detail by Strunge et al. [6] but contributes possible process outcomes when using different experimental parameters. However, the chosen process parameters might not necessarily lead to the theoretically achievable carbonation degrees of the mineral resources. The results serve as a basis for carrying out the carbonation process on an industrial scale, possibly even as a continuous process in the future. To contribute to these goals, e.g., test run durations are limited in time.

The degradation of silicates under formation of carbonates can be described by the carbonation process, which in this study takes places in an

* Corresponding author.
*E-mail address:* kremer@amr.rwth-aachen.de (D. Kremer).

https://doi.org/10.1016/j.jcou.2022.101928
Received 14 October 2021; Received in revised form 25 January 2022; Accepted 6 February 2022
Available online 15 February 2022

agitated autoclave with defined pressure, temperature and stirring speed. The use of an autoclave, or pressure reactor, is necessary to counteract the evaporation and lower $CO_2$ solubility that occurs in an open system due to the increased process temperature. The carbonation process is quite complex because numerous reactions are involved. The reactions are independently influenced by a wide range of process parameters such as temperature, *p*H value and pressure, but also influence one another in order to form carbonates from $CO_2$ and a solid input material. As a first step $CO_2$ needs to dissolve in water, then react with the solvent to generate carbonic acid ($H_2CO_3$) which subsequently dissociates into a hydrogen ion and hydrogen carbonate ($HCO_3^-$) according to the following Eq. (1) [7]:

$$CO_2 + H_2O \quad \leftrightarrow H_2CO_3 \quad \leftrightarrow H^+ + HCO_3^- \tag{1}$$

Each of these three intermediate reactions must be influenced towards the product side for a successful carbonation process. Considering all dependencies of these reversible intermediate reactions, a successful supply of a sufficient amount of $HCO_3^-$ is directly dependent on the $CO_2$ partial pressure of the system and the *p*H value of the solution [8].

In addition to the carbon source, a divalent metal cation is necessary for the formation of the solid carbonates. Hydrolysis of a solid input material transfers the required cations into solution making them available for the carbonation reaction. This reaction is given in Eq. (2) with forsterite ($Mg_2SiO_4$) as a solid, which is one end-member of the olivine solid solution series $(Mg,Fe)_2SiO_4$, and abundant natural mineral [9–11].

$$Mg_2SiO_4 + 4H^+ \rightarrow 2Mg^{2+} + SiO_2 + 2 \quad H_2O \tag{2}$$

In Eq. (2) the intermediate formation of silicic acid is omitted for simplification. Finally, depending on the *p*H value, the hydrogen carbonate deprotonates according to Eq. (3) [12], whereby the released metal cation can react with the new generated carbonate anion to form a carbonate, which precipitates as a solid at a corresponding supersaturation (Eq. 4) [3].

$$HCO_3^- \leftrightarrow CO_3^{2-} + H^+ \tag{3}$$

$$Mg^{2+} + CO_3^{2-} \quad \leftrightarrow MgCO_3 \tag{4}$$

Although hydrogen carbonate is consumed in this reaction, new $HCO_3^-/CO_3^{2-}$ is constantly generated if the $CO_2$ partial pressure is sufficient and, thus, the net carbonation reaction (Eq. 5) is maintained [13].

$$Mg_2SiO_4 + 2CO_2 + H_2O \rightarrow 2MgCO_3 + SiO_2 + \quad H_2O \tag{5}$$

Previous research can be divided into theoretical modelling and assumptions as reported by Bremen et al. [14] and Rimstidt et al. [15] but also into experimental observations consisting of investigations of the different parameters on direct mineral carbonation (see Table 1). The

**Table 1**
Literature review on the effect of parameter variations on the carbonation.

| Process conditions | Results | Ref. |
|---|---|---|
| Pressure, *p*H, dissolution | The *p*H value in contact with the mineral surfaces is the major faction controlling the dissolution rates. | [16] |
| Pressure, temperature, retention time, *p*H, additives, particle size, surface activation, passivation layer, dissolution, precipitation, | Proposed direct carbonation process: 185 °C, 150 bar, addition of 0.64 M $NaHCO_3$ and 1 M NaCl in aq. Decrease in particle size enhances the dissolution of the silicate and the carbonation efficiency. Increasing pressure leads to higher RX. Residence time of 2 h and a neutral *p*H is proposed. Mechanical activation is not recommended due to the high energy demand. | [19] |
| Pressure, temperature, retention time, *p*H, additives, particle size, dissolution, nucleation | The precipitation of magnesite is apparently limited by the process of nucleation. Magnesite precipitation occurs most rapidly in the presence of initial magnesite nuclei. A sufficient supersaturation of conditions is necessary to initiate nucleation, which is the rate-limiting step before precipitation occurs. | [17]. |
| Pressure, temperature, retention time, additives, particle size, passivation layer | $P_{CO2}$ has a minor effect on efficiency than variation of temperature, particle size, $HCO_3^-$concentration and ionic strength in solution. With high addition of sodium salts and high $P_{CO2}$ the rate of carbonation was controlled by chemical reaction between $H^+$ and olivine, but at low $P_{CO2}$ the carbonation was controlled by diffusion through the carbonate layer. Addition of sodium bicarbonate can increase the ionic strength and aid the dissolution of Si followed by decomposition to amorphous silica with a removal of the Si-rich layer. | [23] |
| Pressure, *p*H, additives | Olivine minerals dissolve more rapidly in the presence of organic ligands. The silica dissolution reaction occurs at the mineral surface. | [24] |
| Temperature, *p*H, particle size, surface activation, amorphisation, dissolution | Mechanical activation increases the specific reaction rate by a factor of three compared to inactivated samples. No correlation was found between the particle size and the rate of dissolution. | [25] |
| Temperature, dissolution, precipitation | A direct relation of the reaction mechanism to the stoichiometry was assumed, deriving a simple equation for dissolution and precipitation of silica phases with the result of a direct proportionality of the reaction rate to the interfacial area between the solid and aqueous phases and an inverse proportionality to the mass of water in which the silica is dissolving, indicating that the reaction rates are limited by the breaking of the strong Si-O bonds. | [15] |
| Retention time, additives, particle size, passivation layer, dissolution | Different solutions have been proposed to increase the carbonation extent, like the use of additives, the use of ultrafine particles (below 10 μm) or the application of strong turbulence intensity to avoid the formation of the passivation layer. | [14, 26–28] |
| *p*H, dissolution | Temperature has no influence on the enthalpie of activation. The variation of forsterite dissolution changes with *p*H. At high *p*H, detachment of silicon controls silicate dissolution rates. At low *p*H, detachment of other cations than silica controls dissolution rates of silicates. | [29,30]. |
| *p*H, additives, dissolution | Olivine minerals dissolve more rapidly with declining *p*H. At low *p*H, olivine minerals release cations more rapidly than silica and produce a silica-enriched surface. | [31–34] |
| Particle size, surface activation, amorphisation | Reactivity increased most significantly as a result of size reduction. But it is suggested that structural disordering (amorphisation) through intensive (attrition-type mill) and long milling increases the reactivity over-proportionally. This indicates an activation of olivine by lattice defects. A mechanically-induced increase of the dislocation density is related to an increase in elastically stored energy in the crystal. | [35–41] |
| Passivation layer, in-situ milling | A silica-rich passivation layer inhibits the carbonation reactivity. Importance of particle-particle interactions (abrasion) for generation of fresh olivine reaction surfaces and for extent of carbonation is described. Addition of abrasive particles (e.g. quartz) leads to an increase in carbonation. | [18] |
| Dissolution | The olivine content in the impure samples is proportional to the mineral carbonation (MC) efficiency. The carbonation is kinetically controlled by the chemical reaction of the dissolution of olivine. | [42] |

dissolution of forsterite is mainly controlled by the *p*H value in contact with the mineral surfaces [16]. Various studies show a strong influence of the *p*H value, pressure, temperature, presence of additives, particle size, or the reactive surface on the extent of carbonation. Also, the amorphisation of silicate feed material by intensive milling shows positive effects on the carbonation degree. The precipitation of the reaction product magnesite is limited by the process of nucleation [17]. Another reaction-limiting obstacle is the reaction product amorphous silica on the silicate particles, which inhibits further dissolution and, therefore, acts as a passivation layer. Béarat et al. [18] describe the idea of particle-particle interaction for the generation of fresh olivine reaction surface by addition of abrasive particles (e.g. quartz) to enhance the degree of carbonation by reactivating the surface during carbonation. O'Connor et al. [19] conducted extensive research and proposed parameters for a direct carbonation process, which formed the basis for further studies.

Oelkers et al. [20] describe increasing surface area or extremely acidic conditions as the only pathways to significantly accelerate forsterite dissolution, which is necessary to enhance the carbonation reaction in aqueous solution.

To further improve the process of mineral carbonation, this study examines and compares the effects of parameter variations on the carbonation degree of olivine. A basis is provided for parameters such as temperature, pressure, additives, stirring speed and other parameters that are part of various examinations in literature.

Investigations have been carried out for parameters that have not yet been sufficiently considered. Very narrow particle size distributions with six fractions in the range between 0 and 63 μm are tested to determine the effect of increased surface area on the carbonation. The residence time in the batch autoclave is examined to investigate the effect of time on the crystal growth of the reaction products by means of SEM. The nucleation is assessed by the addition of magnesite into the reactor. The increase in reactivity by continuous liberation of the reactive surface area and the abrasion of the passivation layer is tested by adding ceramic beads to the feed. The carbonation tests are continuously monitored for pressure and temperature and the reaction products – after filtration and drying – are characterised with X-ray fluorescence (XRF), X-ray diffraction (XRD), Differential thermal analysis (DTA)/ Thermogravimetric analysis (TG) and Scanning electron microscope (SEM) to determine the reacted phases, the morphology, the degraded silicates and the carbonation degree.

There are various ways of calculating the degree of carbonation by taking into account either the amount of reactive metal oxides of magnesium, calcium and iron, or simply of magnesium oxide or the amount of forsterite resulting in different carbonation degrees. In the following study, the carbonation degree in wt% is calculated by considering the amount of Mg, Ca and Fe oxides. Additionally, the amount of stored $CO_2$ per tonne of olivine is presented which is independent of the calculation method.

The aim of this study is to provide the optimum parameters for achieving the maximum yield of reaction products. Subsequently, the reaction products are to be used as substitutes in order to improve the overall $CO_2$ balance through the substitution credit. The amorphous silica can be used as a pozzolanic material in a blended cement. The magnesium carbonate can be used as a filler for paper or polymers [21,22].

In order to achieve the maximum reaction yield, we conducted several series of experiments with adjusting only one parameter respectively. After evaluating and calculating the results, further experiments with combinations of promising parameters were carried out. The selected parameter settings are examined in more detail for the first time in this study.

## 2. Materials and methods

### 2.1. Material and sample preparation

The feed material for this parameter study is a peridotite from Aheim Gusdal Mine in Norway [43], the most important deposit of olivine in the world with the producers Sibelco and Steinsvik Olivine AS, which is used for this work. The following phase composition of this material (Table 2), which is commonly named olivine – and is therefore hereinafter referred to as olivine – results in mineralogical classification as peridotite as it is described by Kremer et al. [44–46] Also more information about the geological settings of the deposit are given.

**Table 2**
Mineral composition of olivine feed material based on semi-quantitative XRD determination.

| Mineral Phase Fraction | Feed material [%] |
|---|---|
| Forsterite | 75 – 80 |
| Enstatite | 10 – 15 |
| Lizardite | ≤ 5 |

The feed material was procured with an initial particle size of < 8 mm. In order to obtain different particle size fractions for the carbonation tests, the feed material has been milled with a vertical roller mill (LM3, 6/4, Loesche GmbH, Düsseldorf, Germany) followed by direct classification in the milling chamber by an air classifier (LSKS6, Loesche GmbH, Düsseldorf, Germany) into the two particle size fractions < 20 μm and < 63 μm. A vertical roller mill was used as it is a common aggregate in cement plants and its throughput is high enough to produce sufficient material for later large-scale carbonation tests. The milled olivine material < 20 μm was subsequently sieved wet (AS 200, Retsch GmbH, Haan, Germany) to generate the particle size fractions < 5 μm, 5 – 11 μm, 11 – 20 μm and the olivine material < 63 μm was sieved to produce the particle size fractions 20 – 32 μm, 32 – 45 μm and 45 – 63 μm. The different particle size fractions showed no significant change in composition.

### 2.2. Experimental procedure – carbonation in autoclave

The carbonation tests have been performed in a 1.5 L autoclave (Type 3E Büchi Kiloclave, Büchi AG, Uster, Switzerland) at defined basic parameters as presented in Table 3.

For each tests 1 L of deionised water was filled into the autoclave (Fig. 1), followed by 125 g of the olivine sample and the additives (53.76 g sodium bicarbonate, 5.04 g oxalic acid (dihydrate), 1.76 g ascorbic acid). The autoclave was closed and the stirrer was set to 600 rpm. $CO_2$ was injected until an initial pressure of 30 bar was reached. As a part of the $CO_2$ is going into solution, the pressure was stabilised by repeated injection of $CO_2$ until no losses of pressure could be detected. The autoclave was heated up to 175 °C at a rate of 10 K/min and kept at this temperature for 2 h, followed by cooling down to 25 °C, which was close to the ambient temperature of the plant in the laboratory. The cooling down took about 1.5 h with decreasing cooling rate.

**Table 3**
Basic parameters for carbonation tests.

| Experimental parameters | |
|---|---|
| **Temperature:** | 175 °C |
| **Pressure:** | $p_0$ = 30 bar, $p_{max}$ = ~60 bar |
| **Stirring speed:** | 600 rpm |
| **Heating rate:** | 10 K/min |
| **Cooling rate:** | 50 K/min (max.), decreases exponentially |
| **Retention time:** | 2 h |
| **Solid/liquid ratio:** | 1: 8 |
| **Particle Size:** | < 20 μm |
| **Additives:** | 0.64 M sodium bicarbonate<br>0.04 M oxalic acid<br>0.01 M ascorbic acid |
| ***p*H of solution:** | 8 – 8.5 |

**Fig. 1.** Büchi Kiloclave in operation.

Subsequently, the remaining pressure was released and the autoclave was opened. The solution was pumped out of the autoclave and filtered with a vacuum filter before drying of the solids, whereas a sample of the solution was taken for ICP analysis.

After drying of the solid carbonation product, it was weighed and split to samples for analyses (XRD, XRF, DTA/TG, SEM). The following parameters have been investigated during the carbonation tests (Table 4).

**Table 4**
Investigated parameters during the carbonation tests.

| Investigated parameters during carbonation | |
|---|---|
| **Particle size:** | ▪ < 5 µm<br>▪ 5 – 11 µm<br>▪ 11 – 20 µm<br>▪ 20 – 32 µm<br>▪ 32 – 45 µm<br>▪ 45 – 63 µm |
| **Retention time:** | ▪ 0.5 h[[parms resize(1),pos(50,50),size (200,200),bgcol(156)]]4 h |
| **Addition of ceramic beads:** | ▪ Addition of 50 g ceramic balls (⌀ 2.2 mm)<br>▪ Basic carbonation conditions |
| **Nucleation:** | ▪ Addition of 12.5 g pure magnesite in two different fractions (15 – 20 µm, 45 – 63 µm)<br>▪ Basic carbonation conditions |
| **Combination of parameters:** | ▪ Addition of ceramic beads, 4 h<br>▪ Addition of magnesite seed crystals 15 – 20 µm, 4 h<br>▪ Addition of ceramic beads and magnesite seed crystals 15 – 20 µm, 4 h |

## 2.3. Characterisation

### 2.3.1. Determination of surface area (AREA-meter)

The measurement of the specific surface area was performed with the single-point differential method according to Haul and Dümpgen using AREA-Meter according to DIN 66132. It is a simplified form of the method (BET) developed by Brunauer, Emmet and Teller to measure the amount of nitrogen adsorbed on the inner surface of a powder by the pressure difference of the gas at room temperatures and at − 196 °C (liquid nitrogen).

### 2.3.2. Scanning Electron Microscopy (SEM)

The documentation of the input materials' initial state, examination of the products' microstructure for any abnormalities due to the varied experimental parameters and visual validation of further chemical and mineralogical analysis steps, Scanning Electron Microscopy (SEM) was carried out by a ZEISS GeminiSEM500 by Carl Zeiss AG (Oberkochen, Germany). Additionally, Energy Dispersive X-ray Spectroscopy (EDS) was carried out by an X-Max 80 detector and AZtec software by Oxford Instruments (Oxon, England) to reveal local chemical variations and to selectively analyse the element composition of the formed products.

### 2.3.3. XRF characterisation and loss of ignition determination

To determine the loss on ignition (L.O.I.) values of both the input and output materials of all carbonation trials presented in this study, 2 g of each sample is annealed for 2 h at 1050 °C and balanced after cooling. Especially with regard to the samples having passed the autoclave treatment, the L.O.I. may provide additional information about the carbonation success.

To prepare glass disks for the subsequent chemical analysis via X-ray fluorescence (XRF), 1 g of each sample is transferred to a platinum crucible and fused by a Claisse LeNeo fusion instrument by Malvern PANalytical B.V. (Eindhoven, Netherlands). Eventually, the received glass disks are analysed via XRF utilising a PW2404 device by Malvern PANalytical B.V. (Eindhoven, Netherlands) to obtain the chemical composition.

### 2.3.4. XRD characterisation

To analyse the present mineral phases of the input materials as well as the carbonation products, X-ray diffraction (XRD) technique was conducted in Bragg–Brentano geometry employing a Bruker D8 Advance device by Bruker AXS (Karlsruhe, Germany) equipped with LynxEye detector, CuKα tube and nickel filter. The chosen measuring range from 5° to 90° 2θ was scanned in 0.02° steps at a rate of 2s per step. As this study also aims at a quantitative comparison of the present and formed mineral phases respectively, a subsequent semiquantitative evaluation of the mineral phase composition was executed.

### 2.3.5. TG/DTA determination

Thermal gravimetric and differential thermal analysis were performed using STA 449 F3 Jupiter® and Proteus Thermal Analysis 8.0.2 software by NETZSCH-Gerätebau GmbH, Selb, Germany. Analysis runs were carried out using $Al_2O_3$ crucibles, in a temperature range from 23 °C to 1000 °C with a heating rate of 10 K/min and were performed under argon with a gas flow of 50 ml/min each.

### 2.3.6. Calculation of carbonation degree

Calculation of carbonation degree is based on the Mg, Ca and Fe content of the used olivine and where necessary of single particle size fractions. The element contents are considered independent of the mineralogical phase. The carbonation efficiency is then determined using the following Eq. (6).

$$Carb.\quad Eff.\quad [\%] = \left(\frac{n(CO_{2\quad stored})}{n(Mg + Ca + Fe)}\right) * 100 \tag{6}$$

The mass of stored $CO_2$ for all calculations is based on the L.O.I. of XRF analyses of fully dried samples and are verified over TG/DTA analyses.

For all trials with addition of magnesite crystals the $CO_2$ content of the material is excluded, where the $CO_2$ amount is based on Mg content of the used magnesite and therefore on the maximum amount of $MgCO_3$ in the seed crystals.

#### 2.3.7. Determination of amorphous silica

The amorphous silica content cannot be analysed directly and is therefore determined indirectly and in duplicate. First, arithmetically by means of stoichiometry and secondly by means of a combination of the existing analyses. The calculated results are subject to inaccuracies in the analyses and can therefore vary by a few percent.

The carbonation reaction (Eq. 5) of forsterite as a reactive phase in olivine results in the reaction products magnesium carbonate (two moles) and amorphous silica (1 mol) [47–51].

The magnesium carbonate content is determined by semi-quantitative XRD analysis and DTA/TG. By calculating the molar masses of the reaction products of the stoichiometric Eq. (5), the proportion of amorphous silica in relation to the magnesium carbonate can be approximately calculated. This calculation shows that the content of amorphous silica is about 35.6% of the magnesium carbonate, which means that a total of 73.7% of the reaction products consist of magnesite and about 26.3% of amorphous silica.

The second method carried out for the double determination of the amorphous silica consists of the silicon content from XRF analyses and the phase composition given by semiquantitative XRD analyses. The silicon content of the minerals contained is calculated via the structural formula and the molar masses. By multiplying the quantified and therefore crystalline phases with the respective silicon content, the crystalline silicon content can be determined. This is now subtracted from the total silicon content from the XRF, resulting in the theoretical amorphous silicon content.

The results of these two calculating methods are compared with each other, resulting in differences of total amorphous silica value of maximum 2%.

## 3. Results and discussion

The carbonation of olivine results in the formation of magnesite and amorphous silica (Fig. 2) as it can be described by the sum of partial reactions (Eq. 5), which contains the magnesium silicate – here forsterite – as the reactive component under addition of carbon dioxide to form magnesium carbonate and amorphous silica [3,49].

Previous studies showed specific particle sizes for the reaction products of $< 25$ µm for magnesite and ~20 nm for amorphous silica [52,53]. The SEM images for the obtained carbonation products in this study show different specific particle size fractions of 3 – 5 µm for magnesite and 100 – 200 nm for amorphous silica [5].

These specific particle sizes are constant, regardless of the process conditions. The precipitation of magnesite and silica, which is dependent on *p*H and temperature, results in the formation of euhedral magnesite crystals and a passivation silica layer on the surface of the unreacted olivine slowing down the dissolution and, therefore, also the carbonate formation while reducing the carbonation efficiency [4,18].

It was observed that the magnesite forms on the surface of the unreacted olivine particles and the amorphous silica mainly forms as a passivation layer on the olivine but some silica particles can also be found around the outer edges of the magnesite crystals. The amount of amorphous silica was calculated for the carbonation products ranging from 1.75% to 19.4%. All carbonation tests described below were carried out in duplicate to ensure the results' consistency. The presented figures are average values.

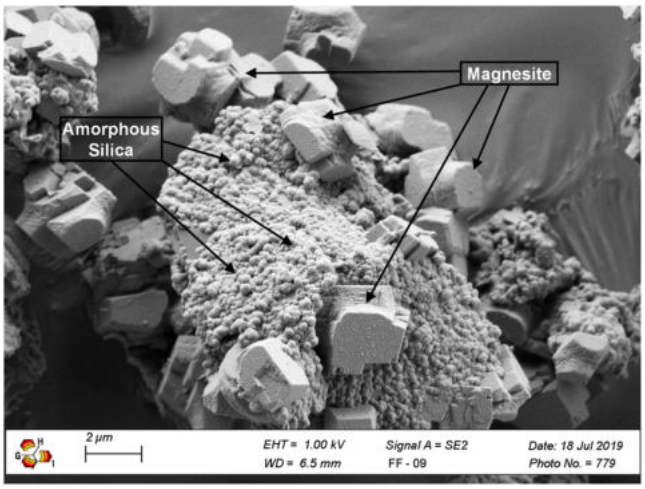


**Fig. 2.** SEM image of carbonation product for olivine $< 20$ µm under previously defined basic carbonation conditions. The reaction products magnesite and amorphous silica are indicated [5].

### 3.1. Particle size

The BET measurements of the six initial particle size fractions before carbonation show an exponential dependence of the specific reaction surface on the particle size fraction used. The fractions from 45 – 63 µm to 11 – 20 µm exhibit no relevant increase in specific reaction area and vary between 0.4 and 0.5 $m^2/g$. Only in the fractions 5 – 11 µm and $< 5$ µm the specific surface area increases significantly, corresponding to a relative increase by a factor of 2.6 and 3.7, respectively. The degree of carbonation of the tests with varying particle size fraction also shows an exponential dependence on the used size fraction, resulting in higher carbonation degrees with decreasing particle size. Thus, a maximum carbonation degree of an average of 21.6% could be achieved within the fraction $< 5$ µm, whereas only 2 – 3% was achieved with all other fractions. Both the specific surface area and the degree of carbonation as a function of the grain size fraction are displayed in Fig. 3.

From these results it can be deduced that the carbonation efficiency increases with increasing specific reaction surface area, which is consistent with literature. Contrary to initial assumptions, however, there is no linear correlation between these two parameters, but an exponential dependence of the carbonation efficiency on the specific surface. Furthermore, it has been reported that an increased amorphised fraction of mechanically agitated material to the feed stock has a positive influence on carbonation, which can neither be confirmed nor

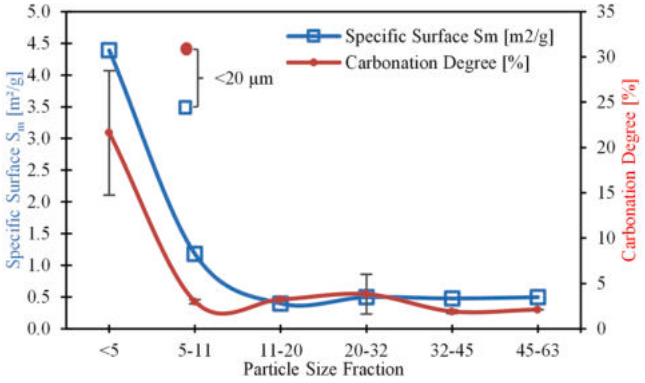


**Fig. 3.** Effect of differing particle size or specific surface area on carbonation degree. The six consistent particle size fractions are presented and linked in relation to the degree of carbonation and the specific surface area. The fraction $< 20$ µm is stated separately.

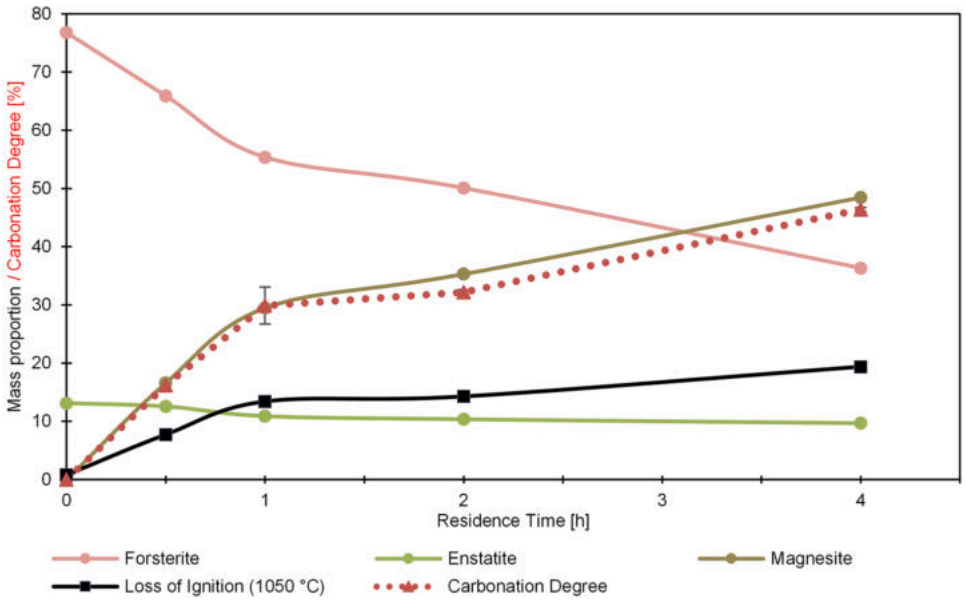


**Fig. 4.** Effect of varying residence time on phase composition and carbonation degree. Phase composition plotted as functions of time. Loss of ignition does not belong to the phase composition but serves as an indicator for the carbonation success. The carbonation degree is drawn in dots. The composition at 0 h is the initial olivine < 20 μm prior to carbonation experiments. Four experiments have been examined at the residence times 0.5 h, 1 h, 2 h and 4 h. Trend lines are added to aid data visualization.

refuted in the context of this study due to a lack of data in this regard [25,35–41].

In the context of particle size influence, it was noticed that with the fraction < 20 μm a higher carbonation efficiency of 32.2% was achieved than with the fraction < 5 μm, despite a lower specific reaction surface. From this result it can be concluded that in the fraction < 20 μm a stronger particle-particle interaction takes place, which keeps the reaction surface of the olivine active due to the impact of larger or heavier particles and therefore enhancing the carbonation reaction. Béarat et al. [18] reported similar observations in this regard.

### 3.2. Retention time

The effect of varying retention time was examined by carbonation of the particle size fraction < 20 μm for four different times. The carbonation degree increased with a longer residence time in the reactor. Fig. 4 shows the behaviour of the carbonation degree as a function of the retention time, which is very steep in the first hour of the carbonation and then flattens out to a quasi-linear progression up to 4 h. Longer retention times were dispensed with due to economic efficiency and because of the subsequent planning of continuous operation. At the maximum retention time of 4 h, a relative increase of 44.1% was achieved compared to the standard of 2 h, with an absolute degree of carbonation of 46.4%.

At the beginning of the carbonation the whole reactive surface of the olivine is free, which allows the dissolution of the magnesium silicate and therefore a comparatively high reactivity. After some time, a passivation layer has been built upon the reactive surface inhibiting the reaction. This passivation layer is continuously destroyed by the impact of coarser particles in the fraction < 20 μm, regenerating reactive surface, which results in a nearly linear progression of the carbonation degree for a longer retention time.

Due to the nature of orthosilicates, the $SiO_4$ tetrahedra are not linked to each other. Depending on the *p*H regime, the addition to an aqueous solution causes a reaction to $Si(OH)_4$ or, in case of more basic milieus, to $Si(OH)_3O^-$. Due to polycondensation of the beforementioned monomers, accompanied by splitting off a water molecule, monosilicic acid forms disilicic acid. Via various intermediates, silica eventually occurs in an amorphous state [54–56].

Fig. 5 illustrates the independent formation of silica and magnesite depending on the retention time. In the lower right corner of the SEM picture detail after 0.5 h (a), not only magnesite growth is visible but also silica formation on the edges of the just evolved magnesite. After 2 h, the independent formation of silica and magnesite is emphasized: If the magnesite crystals are of sufficient size, they begin growing around the silica particles or even enclose them after 4 h of retention time, as depicted in Fig. 5c), which presents a major challenge for the subsequent separation process. However, the reverse case was also observed: After 4 h, magnesite surfaces were also almost completely covered with silica particles (Fig. 5d)).

### 3.3. Addition of magnesite seed crystals

Since, in addition to the amorphous silicon, the forming magnesite crystallises on the input material and thus inhibits further carbonation, seed crystals of pure magnesite were used to offer the newly forming crystals an energetically more favourable surface and to keep the surface of the olivine clean. This could also lead to positive results for the subsequent separation of the carbonation products as preparation for application. The magnesite crystals that form during carbonation, which typically have a size of 3 – 5 μm, crystallise on the coarser seed crystals and can thus be separated from the amorphous silica (100 – 200 nm) by means of classification [5,57]. The influence of two seed crystals differing in grain size on carbonation were tested, 45 – 63 μm and 15 –

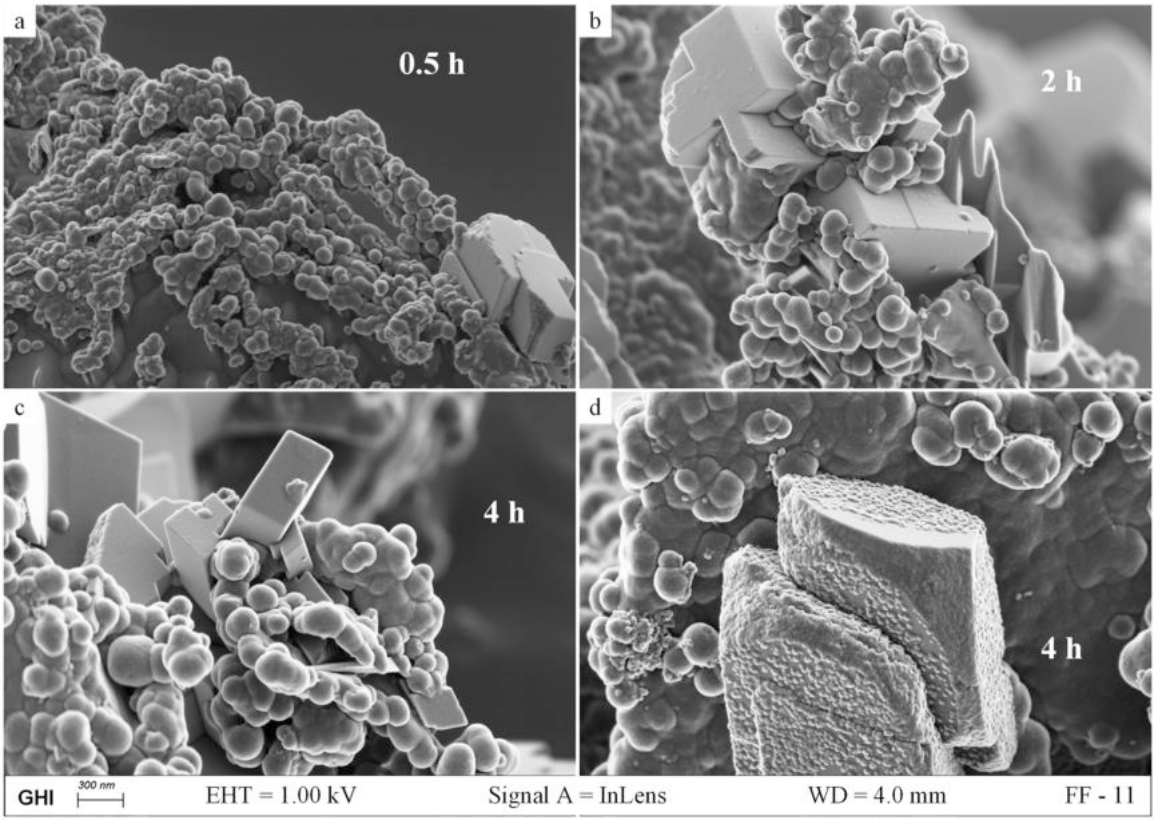


**Fig. 5.** SEM images (30,000 x magnification) of the reaction products sorted according to the retention time. The magnesite particles can be identified by their rhombohedral crystal faces. The amorphous silica is characterised by spherical particles. The magnesite crystals and the amorphous silica are mainly located on the surface of unreacted olivine particles, but are also visible as intergrown particles, which makes subsequent separation challenging.

20 μm, respectively. All other parameters were kept constant as shown in Table 3. The resulting carbonation degree compared to the 2 h basic trial without using seed crystals is visible in Fig. 6. By using seed crystals with particle sizes of 45 – 63 μm and 15 – 20 μm, a relative increase in carbonation degree of 19% and 37.9%, respectively, was achieved, resulting in a total carbonation degree of 38.3% and 44.3%, accordingly.

When determining the carbonation degrees, it should be noted that the amount of added magnesite was excluded in order to include only newly formed carbonate phases. Therefore, a direct confirmation of the carbonation degree by means of DTA/TG is not possible. However, the values of the total magnesite degradation are in agreement, taking the added magnesite into account. The aim of improving the carbonation degree by adding magnesite as seed crystals could therefore be achieved. Parts of the newly formed magnesite crystallised on the surface of the seed crystals, as confirmed by the SEM analysis shown in Fig. 7b). However, crystallisation on the olivine could not be avoided completely (see Fig. 7c)), but according to the results, a strong passivation of the material could be avoided, so that an unhindered reaction of the olivine was possible for a longer period of time. This assumption is based on a work of Stockmann et al. [58] regarding calcite crystallisation on seed crystals. Following earlier publications by Rodriguez-Blanco et al. [59], Hu et al. [60], and Teng [61], Stockmann et al. [58] assumed that calcite nucleation proceeds according to the classical nucleation theory. Therefore, the nucleation proceeds by attaching single ions and not through an accumulation of previously formed clusters in solution [62]. Considering the formation of magnesite in this study comparable to that of calcite and that both minerals are chemically and mineralogically similar, this should allow the assumption that the classical nucleation theory is also applicable here. In addition to supersaturation, this type of nucleation is determined by interfacial energy [63]. The interfacial free energy, in turn, becomes low when the crystal structure of the crystallisation surface is fairly similar to one of the crystal plane of the nucleus [64]. This seems to be the case with olivine, so that the thermodynamic barrier for magnesite nucleation on the olivine surface is relatively low. Thus, a complete avoidance of a magnesite deposition on the olivine by adding magnesite as seed crystals is not possible. However, magnesite deposition will take place on the seed crystals before crystallisation on olivine, as it is energetically more favourable because of matching crystal planes. Subsequent primary grain growth takes place, which requires even less energy than magnesite nucleation. This circumstance

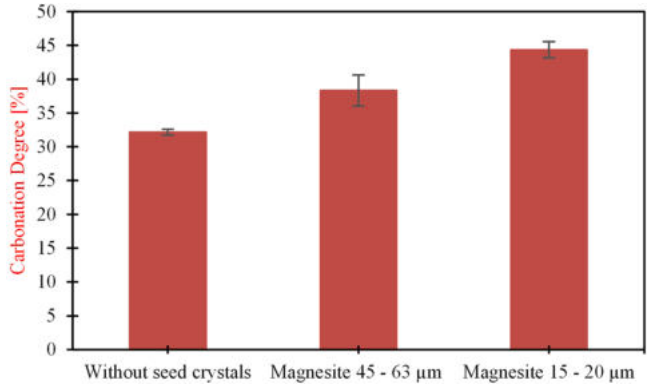


**Fig. 6.** Influence of magnesite seed crystals. The left column presents the carbonation degree at a retention time of 2 h without seed crystals, and the others with the addition of magnesite in two different particle size fractions.

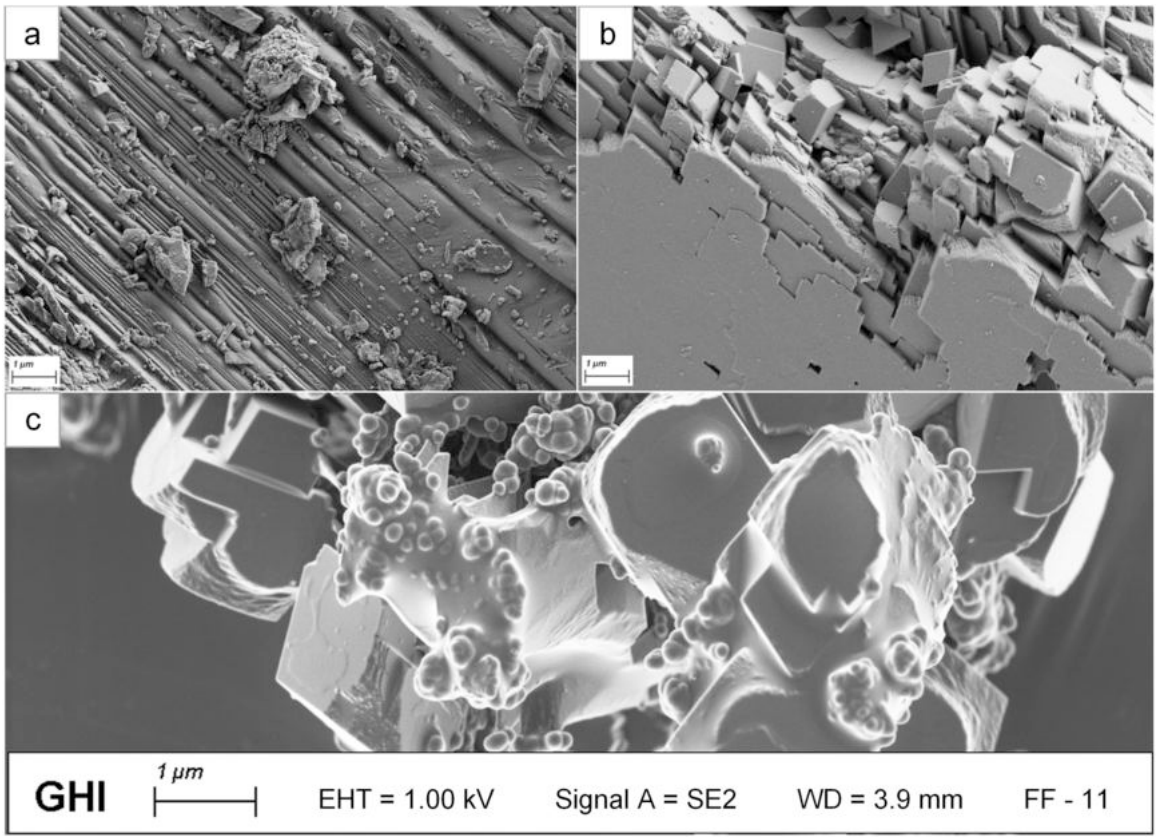


**Fig. 7.** SEM images (10,000 x magnification) of the effect of nucleation with magnesite; (a) unreacted magnesite seed crystal 45 – 63 µm; (b) Carbonation of olivine < 20 µm with addition of magnesite seed crystals (45 – 63 µm) at basic parameters – fraction > 45 µm; (c) Carbonation of olivine < 20 µm with addition of magnesite seed crystals (45 – 63 µm) at basic parameters – fraction < 20 µm.

results in the deceleration of the strong olivine passivation by magnesite crystallisation due to a lower overall supersaturation and therefore in a higher carbonation degree. This assumption also corresponds to the results regarding the use of different particle sizes of the seed crystals. By using smaller seed crystals, a larger specific surface area is available for the energetically lower nucleation and primary magnesite growth, so that greater supersaturation and associated crystal formation on the olivine can be better prevented, which in turn also leads to increased carbonation degree.

Fig. 7c) shows the fraction < 20 µm after carbonation for 2 h with addition of coarse magnesite crystals. In contrast to previous SEM images the clear edges of the magnesite crystals are covered with a magnesite layer, as are the spherical silica particles. This could be a result of post-processing parameters as cooling rate or subsequent filtration and drying with a high amount of magnesium still in solution as precipitation has not been completed.

### 3.4. Addition of ceramic beads

Literature research showed the presence of a passivation silica-rich layer on the reactive surface of the olivine, inhibiting the carbonation reaction. Béarat et al. [18] describe the generation of fresh reaction surface due to particle-particle interaction by addition of abrasive particle like quartz into the reactor. Within the framework of this study, it was decided to add ceramic beads into the autoclave. Yttrium stabilised zirconia grinding elements (Netzsch ZetaBeads®) with a diameter of 2.2 mm were used. These inert beads of the chosen size do not themselves participate in the reaction, but should contribute sufficient energy to destroy the passivation layer on the magnesium silicate and generate reactive surface to increase the degree of carbonation. Due to the differences in particle size, the ceramic beads can be removed from the carbonation products by screening. Carbonation tests with addition of ceramic beads have been conducted with basic carbonation parameters with a retention time of 2 h. Fig. 8 shows the carbonation degree of the used olivine at the basic parameters but with varying retention time. In the column depicted for 2 h, the influence of the addition of ceramic beads to the reaction is visible with a rise in reaction rate from 32.2% to 43.2%, which is close to the carbonation degree at basic conditions without ceramic beads for 4 h with 46.4% and corresponds to an increase of 34.1%.

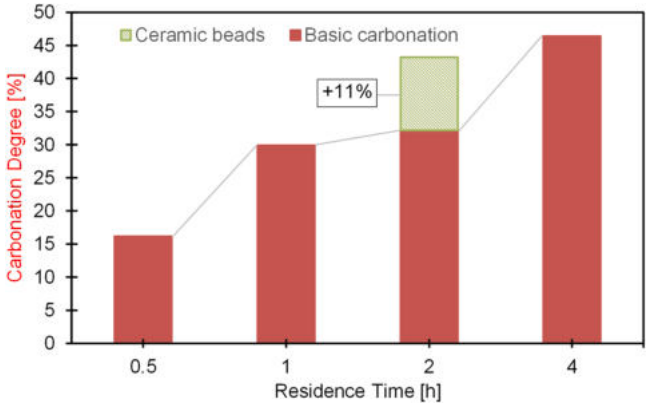


**Fig. 8.** Effect of addition of ceramic beads. The slope in the degree of carbonation is plotted and compared with the different residence times.

### 3.5. Combination of investigated parameters

The parameters studied with regard to the influence on the carbonation degree showed a positive impact of the increase in surface area, respectively increase of the degree of amorphisation. The effect of particle-particle interaction has a significant influence on the reaction and therefore a wider particle size distribution is proposed consisting of very small particles with a large reactive surface area and of coarser particle, which generate a sufficient impact force to break up the passivation layer on the olivine particles and generate fresh reactive surface enhancing the carbonation.

This effect can be supported by the addition of ceramic beads into the reactor. These ceramic beads are inert additives, which do not themselves participate in the reaction, but promote it by generating free reactive surface.

A prolonged retention time has a positive effect on the degree of reaction, which is visible in the almost linear progression of the degree of carbonation with respect to time in Fig. 4.

The highest degree of carbonation that could be achieved in the previously described experiments was 46.4%. The carbonation of olivine $< 20$ μm with a residence time of 4 h showed this maximum reaction rate of 46.4% and the experiment with the addition of ceramic beads for 2 h resulted in a carbonation degree of 43.2%, the addition of magnesite seed crystals led to a reaction yield of 44.3%, respectively. Therefore, to optimise the carbonation and to achieve higher carbonation degrees, further experiments were carried out with the following combinations of parameters:

1. Fraction: $< 20$ μm, 4 h reaction time, addition of ceramic beads
2. Fraction: $< 20$ μm, 4 h reaction time, addition of magnesite seed crystals 15 – 20 μm
3. Fraction: $< 20$ μm, 4 h reaction time, addition of ceramic beads and magnesite seed crystals 15 – 20 μm

The parameter-optimised experiment 1 results in a carbonation degree of ~51% and a $CO_2$ uptake of 259 $kg_{CO2}/t_{olivine}$, which represents a relative increase of ~18% related to the addition of ceramic beads for a reaction time of 2 h or an increase of 10% compared to the reaction for 4 h without ceramic beads. The addition of ceramic beads for 4 h exposes small areas in the surface of the silica passivation layer (see Fig. 9). Thin sharp-edged lamellae are located on the olivine particle surface, on top of which the amorphous silica particles form. SEM images of other carbonation tests showed comparable effects, but to a lesser extent. This could be a result of the dissolution kinetics during the carbonation process. Olivine, especially forsterite-rich olivine is among the fastest dissolving silicate minerals [20,65].

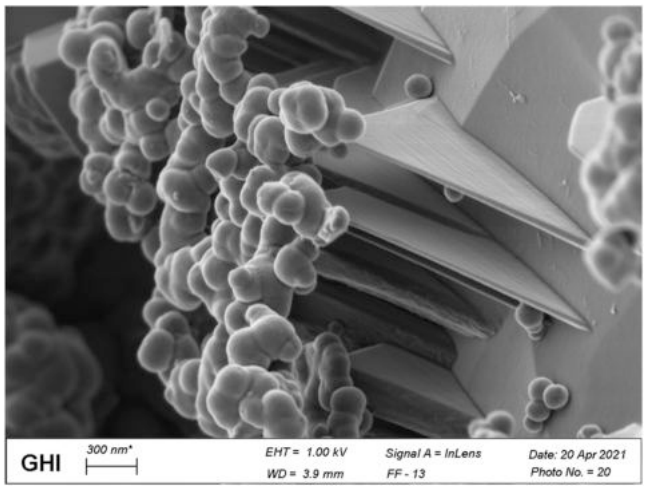


**Fig. 9.** Amorphous silica particles on the tips of the poorly soluble iron mineral lamellae.

Differences in solubility can lead to the retention of poorly soluble crystal structures if the dissolution of the silicates is not complete. Under the conditions in the reactor (slightly basic *p*H, $T = 175$ °C, $p_{max} \approx 60$ bar) it is assumed that the lamellae are insoluble. EDS measurements prove a higher iron content for these lamellae compared the average feed material. It is assumed that the feed material contains iron-rich pyroxenic layers that have a lower solubility under the present conditions and therefore remain stable, while the iron poorer material (e.g. forsterite) dissolves and reacts with the $CO_2$. The texture of this lamellae can be a result of the genesis of olivine-containing rocks. This common constituent of altered ultramafic rocks can also occur as a primary mineral in certain metamorphic rocks [66]. During the formation of igneous and metamorphic rocks exsolution textures or lamellae can be induced by cooling. At high temperatures and high pressures these exsolution lamellae, which were entirely dissolved in their host mineral structures which are mainly ortho- and clinopyroxenes, form fine crystals. Many pyroxenes from terrestrial and extra-terrestrial igneous or mantle rocks show these exsolution textures of thin ortho- or clinopyroxene lamellae [44,67–71]. The content of ortho- and clinopyroxenes in the examined olivine for this study is ~ 13 vol% [44]. During dissolution in the reactor, it is assumed that these lamellae are insoluble under the prevailing conditions, whereas the forsteritic phases dissolve and react with the carbon dioxide as described by the carbonation reaction. As shown in Fig. 9 the amorphous silica particles settle on the edges of the iron-rich lamellae and not on the smooth surface.

Van den Heuvel et al. [72] investigated the precipitation of silica on different surfaces showing that the deposition of silica is mainly controlled by surface morphology. Guha [73] describes the favourable particle deposition along edges resulting in natural obstacles causing a turbulent flow [72,73]. Along surface defects nucleation is also promoted compared to the rest of the surface as it is energetically more favourable [74]. Over time the formed nuclei grow as a result of further silica precipitation leading to the formation of a botryoidal silica layer [72,75,76].

The parameter-optimised experiment 2 results in a carbonation degree of ~60% and a $CO_2$ uptake of 305 $kg_{CO2}/t_{olivine}$, which represents a relative increase of 35.4% related to the addition of magnesite seed crystals 15 – 20 μm for a reaction time of 2 h or a relative increase of 29% compared to the reaction for 4 h without magnesite crystals. As it is visible in Fig. 10 two different things can be observed. The typical image of the carbonation products magnesite and amorphous silica nearly completely enclosing the olivine (Fig. 10b) and the added coarse magnesite particles at 15 – 20 μm with newly formed magnesite crystals as carbonation products. In contrast to Fig. 7c), which displays experiments with a retention time of only 2 h, there are clear crystal surfaces and edges.

The parameter-optimised experiment 3 with a combination of all positive parameters results in a carbonation degree of 48.7% and a $CO_2$ uptake of 248 $kg_{CO2}/t_{olivine}$, which is a slight increase in comparison to the carbonation for 4 h without additives. Nevertheless, the combination of both parameters having proved to be positively affecting the carbonation efficiency in experiments 1 and 2, namely the addition of magnesite and ceramic beads, with a retention time of 4 h results in a lower carbonation degree than both previously described parameter variations. These results do not meet the initial expectations for this set of parameters but should not be disregarded because of its reproducibility. Two possible explanations lie in the solid content present in the reactor chamber on the one hand and the magnesite formation on the other. Adding magnesite for nucleation and simultaneously maintaining the amount of feedstock to be carbonated increases the particle volume in the reactor chamber. This not only allows collisions between the ceramic beads, whose amount also remains unchanged, and the reaction surface of the olivine gradually covered with formed magnesite as well as amorphous silica. It also evokes interaction between the additional

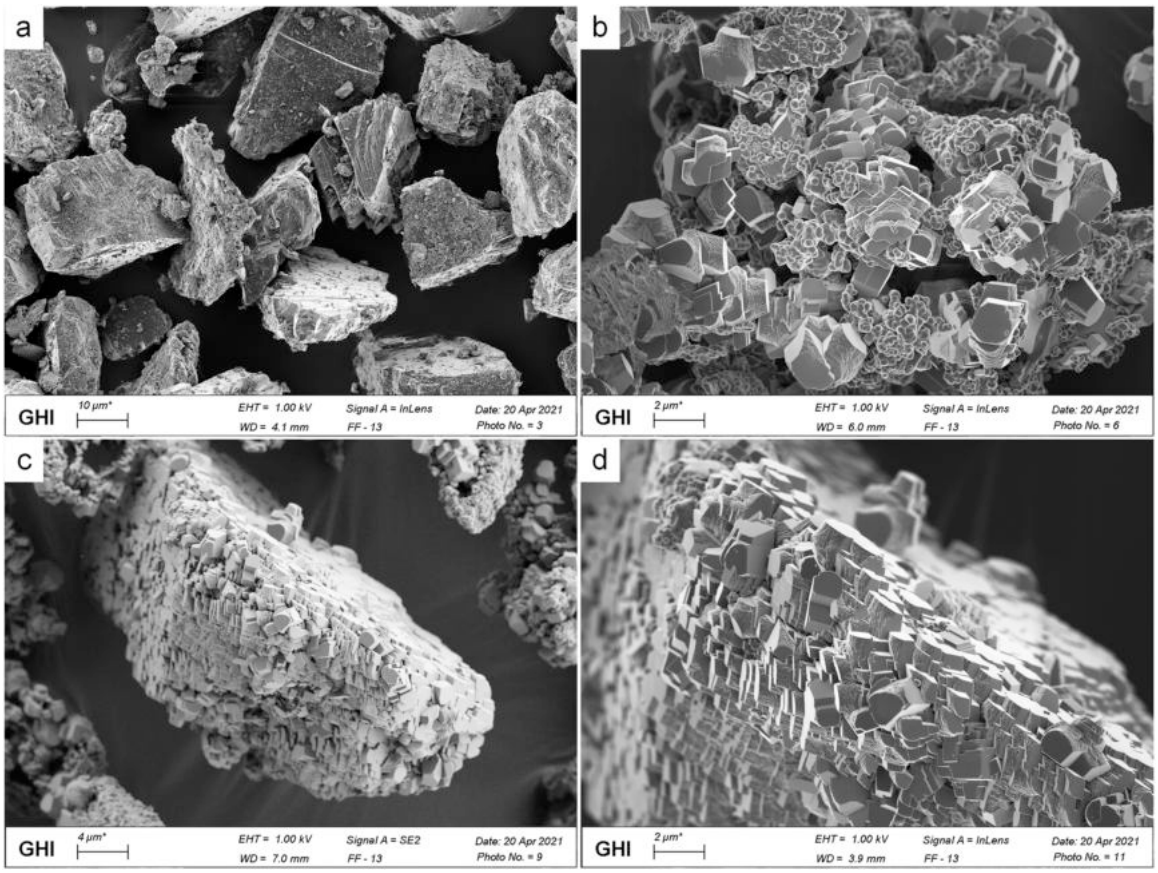


**Fig. 10.** SEM images of reaction products produced by a combination of retention time of 4 h with addition of magnesite seed crystals at 15 – 20 µm. a) Magnesite crystals added before carbonation (magnified by 1000); b) Agglomerate of reaction products magnesite and amorphous silica on the surface of initial olivine particles (x5000); c) Added magnesite crystals after carbonation with only the reaction product magnesite growing on the surface (x2500); d) Added magnesite crystals after carbonation with only the reaction product magnesite growing on the surface (x5000).

magnesite (15 – 20 µm) and the magnesite crystals or silica particles formed on its surface during the corresponding reaction time. This may result in less regeneration of olivine reaction surface compared to experiment 1 due to less probable collisions of ceramic beads and olivine. Furthermore, no interaction between ceramic beads and magnesite was present in experiment 2 and thus, there was no possibility to influence the formation of magnesite on the added seed crystals. As a result of the collisions, a negative influence by also destroying new nuclei on seed crystal surfaces cannot be completely excluded and is assumed to be a partial cause of the significantly reduced carbonation efficiency.

## 4. Summary and conclusions

This study investigated the effect of material and process related parameters on the reaction efficiency for the carbonation reaction. A reaction yield of 60% was achieved, which corresponds to nearly twice the carbonation degree of the previously used basic parameters. The following findings could be made within this parameter study:

(i) The reactivity of the single particles increases with lower particle size or higher surface are. Nevertheless, the overall reaction yield is enhanced by a combination of more parameters. The amorphisation of the particles as a result of mechanical activation and the regeneration of fresh reactive surfaces area are important factors for a high degree of carbonation. Therefore, a broader range for the particle size distribution or the addition of inert beads can have a positive effect to enhance the carbonation reaction.

(ii) The degree of carbonation is increased with higher residence time. However, as the curve flattens, the carbonation rate slows down. Furthermore, the precipitation of the reaction products or the growth of those changes with different reaction times by means of firstly growing of amorphous silica and magnesite mostly separately on the surface of the host material olivine and with increasing retention time forming agglomerates with each other.

(iii) The addition of magnesite as seed crystals enhances the carbonation reaction. The magnesite deposition preferably takes place on the seed crystals instead of crystallisation on the olivine, as it is energetically more favourable and subsequent primary magnesite growth takes place. This circumstance results in the deceleration of the strong olivine passivation by magnesite crystallisation due to a lower overall supersaturation and therefore in a higher carbonation degree.

For the investigated olivine ore with 80% forsterite (magnesium silicate), a theoretical maximum 100% carbonation degree with a $CO_2$ uptake of 508 $kg_{CO2}/t_{olivine}$ was calculated. It was possible to increase the practically achieved degree of carbonation with improved parameters from 32% from previously defined basic parameters to 60%, which corresponds to an increase in carbonation degree of 87.5%. The total $CO_2$ uptake was increased from 166 kg carbon dioxide per tonne of olivine to 305 $kg_{CO2}/t_{olivine}$, which represents an increase of 83.7% in total mass of stored $CO_2$.

## Funding

This research was funded by BMBF (Federal Ministry of Education and Research) in Berlin, grant number 033RCO14B (CO2MIN Project in period from 01.06.2017 to 31.12.2020).

## CRediT authorship contribution statement

**Dario Kremer**: Conceptualization, Methodology, Investigation, Writing – original draft, Visualisation. **Christian Dertmann**: Methodology, Formal analysis, Investigation, Writing – original draft. **Simon Etzold**: Methodology, Formal analysis, Writing – original draft, Validation. **Rainer Telle**: Supervision, Writing – review & editing. **Bernd Friedrich**: Supervision, Writing – review & editing. **Hermann Wotruba**: Supervision Writing – review & editing, Project administration.

## Declaration of Competing Interest

The authors declare that they have no known competing financial interests or personal relationships that could have appeared to influence the work reported in this paper.

## Data Availability

The authors declare that the main data supporting the findings of this study are available within the article. Extra data are available in the supplementary material or from the corresponding author upon request.

## Acknowledgements

We would like to thank our project partners from RWTH Aachen (AVT-SVT, LTT), IASS Potsdam, HeidelbergCement AG and GreenMinerals.

## Appendix A. Supporting information

Supplementary data associated with this article can be found in the online version at doi:10.1016/j.jcou.2022.101928.

## References

[1] United Nations: Climate Change. The Paris Agreement. 2021 United Nations Framework Convention on Climate Change. Available at ⟨https://unfccc.int/process-and-meetings/the-paris-agreement/the-paris-agreement⟩.
[2] IPCC, IPCC Special Report on Carbon Dioxide Capture and Storage. Prepared by Working Group III of the Intergovernmental Panel on Climate Change, Cambridge University Press, 2005, p. 442.
[3] D. Daval, Carbon dioxide sequestration through silicate degradation and carbon mineralisation. Promises and uncertainties, npj Mater. Degrad. 2 (2018) 1677, https://doi.org/10.1038/s41529-018-0035-4.
[4] A. Sanna, M. Uibu, G. Caramanna, R. Kuusik, M.M. Maroto-Valer, A review of mineral carbonation technologies to sequester $CO_2$, Chem. Soc. Rev. 43 (2014) 8049–8080, https://doi.org/10.1039/c4cs00035h.
[5] D. Kremer, H. Wotruba, Separation of products from mineral sequestration of $CO_2$ with primary and secondary raw materials, Minerals 10 (2020) 1098, https://doi.org/10.3390/min10121098.
[6] Strunge, T., Renforth, P. & van der Spek, M. Towards a business case for CO2 mineralisation in the cement industry (2021).
[7] F.J. Roughton, V.H. Booth, The catalytic effect of buffers on the reaction CO(2)+H(2)Oright harpoon over left harpoonH(2)CO(3), Biochem. J. 32 (1938) 2049–2069, https://doi.org/10.1042/bj0322049.
[8] B.J. Krieg, S.M. Taghavi, G.L. Amidon, G.E. Amidon, In vivo predictive dissolution: transport analysis of the $CO_2$, bicarbonate in vivo buffer system, J. Pharm. Sci. 103 (2014) 3473–3490, https://doi.org/10.1002/jps.24108.
[9] Butt, D.P. et al. The kinetics of binding carbon dioxide in magnesium carbonate (1998).
[10] O'Connor, W.K. et al. CO2 Storage in solid form: A study of direct mineral carbonation. Proceedings of the 5th International Conference on Greenhouse Gas, August 2000.
[11] O'Connor, W.K., Dahlin, D.C., Turner, P.C. Walters, R. Carbon dioxide sequestration by ex-situ mineral carbonation. Proceedings of the Second Annual Dixy Lee Ray Memorial Symposium. Albany Research Center, August 29 - September 2, 1999.
[12] T. Umschlag, H. Herrmann, The carbonate radical ($HCO_3$·/$CO_3$··) as a reactive intermediate in water chemistry: kinetics and modelling, Acta Hydrochim. Hydrobiol. 27 (1999) 214–222, https://doi.org/10.1002/(SICI)1521-401X(199907)27:4<214::AID-AHEH214>3.0.CO;2-6.
[13] O'Connor, W.K., Dahlin, D.C., Nilsen, D.N., Walters, R.P. & Turner, P.C. (eds.). Carbon Dioxide Sequestration by Direct Mineral Carbonation with Carbonic Acid (2000).
[14] A.M. Bremen, T. Ploch, A. Mhamdi, A. Mitsos, A mechanistic model of direct forsterite carbonation, Chem. Eng. J. 404 (2021), 126480, https://doi.org/10.1016/j.cej.2020.126480.
[15] J.D. Rimstidt, H.L. Barnes, The kinetics of silica-water reactions, Geochim. Et. Cosmochim. Acta 44 (1980) 1683–1699, https://doi.org/10.1016/0016-7037(80)90220-3.
[16] S.V. Golubev, O.S. Pokrovsky, J. Schott, Experimental determination of the effect of dissolved $CO_2$ on the dissolution kinetics of Mg and Ca silicates at 25 °C, Chem. Geol. 217 (2005) 227–238, https://doi.org/10.1016/j.chemgeo.2004.12.011.
[17] D.E. Giammar, R.G. Bruant, C.A. Peters, Forsterite dissolution and magnesite precipitation at conditions relevant for deep saline aquifer storage and sequestration of carbon dioxide, Chem. Geol. 217 (2005) 257–276, https://doi.org/10.1016/j.chemgeo.2004.12.013.
[18] H. Béarat, et al., Carbon sequestration via aqueous olivine mineral carbonation: role of passivating layer formation, Environ. Sci. Technol. 40 (2006) 4802–4808, https://doi.org/10.1021/es0523340.
[19] O'Connor, W.K. et al. Aqueous Mineral Carbonation. Mineral Availability, Pretreatment, Reaction Parametrics, and Process Studies. Office of Fossil Energy, US DOE, March 15, 2005.
[20] E.H. Oelkers, J. Declercq, G.D. Saldi, S.R. Gislason, J. Schott, Olivine dissolution rates: a critical review, Chem. Geol. 500 (2018) 1–19, https://doi.org/10.1016/j.chemgeo.2018.10.008.
[21] H. Ostovari, A. Sternberg, A. Bardow, Rock 'n' use of CO 2. Carbon footprint of carbon capture and utilization by mineralization, Sustain. Energy Fuels 4 (2020) 4482–4496, https://doi.org/10.1039/d0se00190b.
[22] H. Ostovari, L. Müller, J. Skocek, A. Bardow, From unavoidable $CO_2$ Source to $CO_2$ sink? A cement industry based on $CO_2$ mineralization, Environ. Sci. Technol. (2021), https://doi.org/10.1021/acs.est.0c07599.
[23] F. Wang, D. Dreisinger, M. Jarvis, T. Hitchins, Kinetics and mechanism of mineral carbonation of olivine for $CO_2$ sequestration, Miner. Eng. 131 (2019) 185–197, https://doi.org/10.1016/j.mineng.2018.11.024.
[24] R.A. Wogelius, J.V. Walther, Olivine dissolution at 25°C. Effects of pH, $CO_2$, and organic acids, Geochim. Et. Cosmochim. Acta 55 (1991) 943–954, https://doi.org/10.1016/0016-7037(91)90153-V.
[25] T.A. Haug, R.A. Kleiv, I.A. Munz, Investigating dissolution of mechanically activated olivine for carbonation purposes, Appl. Geochem. 25 (2010) 1547–1563, https://doi.org/10.1016/j.apgeochem.2010.08.005.
[26] L. Turri, H. Muhr, K. Rijnsburger, P. Knops, F. Lapicque, $CO_2$ sequestration by high pressure reaction with olivine in a rocking batch autoclave, Chem. Eng. Sci. 171 (2017) 27–31, https://doi.org/10.1016/j.ces.2017.05.009.
[27] W.J. Huijgen, R.N. Comans, G.-J. Witkamp, Cost evaluation of $CO_2$ sequestration by aqueous mineral carbonation, Energy Convers. Manag. 48 (2007) 1923–1935, https://doi.org/10.1016/j.enconman.2007.01.035.
[28] J. Li, M. Hitch, Mechanical activation of ultramafic mine waste rock in dry condition for enhanced mineral carbonation, Miner. Eng. 95 (2016) 1–4, https://doi.org/10.1016/j.mineng.2016.05.020.
[29] P.V. Brady, J.V. Walther, Controls on silicate dissolution rates in neutral and basic pH solutions at 25°C, Geochim. Et. Cosmochim. Acta 53 (1989) 2823–2830, https://doi.org/10.1016/0016-7037(89)90160-9.
[30] E.H. Oelkers, An experimental study of forsterite dissolution rates as a function of temperature and aqueous Mg and Si concentrations, Chem. Geol. 175 (2001) 485–494, https://doi.org/10.1016/S0009-2541(00)00352-1.
[31] Y. Liu, Mechanism for the dissolution of olivine series minerals in acidic solutions, Am. Mineral. 91 (2006) 455–458, https://doi.org/10.2138/am.2006.2077.
[32] J.J. Rosso, J. Rimstidt, A high resolution study of forsterite dissolution rates, Geochim. Cosmochim. Acta 64 (2000) 797–811, https://doi.org/10.1016/S0016-7037(99)00354-3.
[33] O.S. Pokrovsky, J. Schott, Forsterite surface composition in aqueous solutions. A combined potentiometric, electrokinetic, and spectroscopic approach, Geochim. Et. Cosmochim. Acta 64 (2000) 3299–3312, https://doi.org/10.1016/S0016-7037(00)00435-X.
[34] H. Seyama, M. Soma, A. Tanaka, Surface characterization of acid-leached olivines by X-ray photoelectron spectroscopy, Chem. Geol. 129 (1996) 209–216, https://doi.org/10.1016/0009-2541(95)00142-5.
[35] R.A. Kleiv, M. Thornhill, The effect of mechanical activation in the production of olivine surface area, Miner. Eng. 89 (2016) 19–23, https://doi.org/10.1016/j.mineng.2016.01.003.
[36] R.A. Kleiv, M. Thornhill, Mechanical activation of olivine, Miner. Eng. 19 (2006) 340–347, https://doi.org/10.1016/j.mineng.2005.08.008.
[37] C.A. Summers, D.C. Dahlin, G.E. Rush, W.K. O'Connor, S.J. Gerdemann, Grinding methods to enhance the reactivity of olivine, Min., Metall. Explor. 22 (2005) 140–144, https://doi.org/10.1007/BF03403128.
[38] McKelvy, M.J., Chizmeshya, A., Bearat, H., Sharma, R. & Carpenter, R.W. Developing a Mechanistic Understanding of CO2 Mineral Sequestration Reaction Processes. Proc. 26th International Tech. Conference on Coal Utilization & Fuel Systems. pp. 777–788, March 5–8/2001.

[39] J. Li, M. Hitch, Ultra-fine grinding and mechanical activation of mine waste rock using a high-speed stirred mill for mineral carbonation, Int J. Min. Met. Mater. 22 (2015) 1005–1016, https://doi.org/10.1007/s12613-015-1162-3.
[40] D. Tromans, J.A. Meech, Enhanced dissolution of minerals. Stored energy, amorphism and mechanical activation, Miner. Eng. 14 (2001) 1359–1377, https://doi.org/10.1016/S0892-6875(01)00151-0.
[41] S. Atashin, J.Z. Wen, R.A. Varin, Investigation of milling energy input on structural variations of processed olivine powders for $CO_2$ sequestration, J. Alloy. Compd. 618 (2015) 555–561, https://doi.org/10.1016/j.jallcom.2014.08.142.
[42] F. Wang, D. Dreisinger, M. Jarvis, T. Hitchins, Kinetic evaluation of mineral carbonation of natural silicate samples, Chem. Eng. J. 404 (2021), 126522, https://doi.org/10.1016/j.cej.2020.126522.
[43] Malvik T. (ed.). Industrial Mineral Producers in Norway, 2008.
[44] D. Kremer, et al., Geological mapping and characterization of possible primary input materials for the mineral sequestration of carbon dioxide in Europe, Minerals 9 (2019) 485, https://doi.org/10.3390/min9080485.
[45] A. Streckeisen, To each plutonic rock its proper name, Earth Sci. Rev. 12 (1976) 1–33, https://doi.org/10.1016/0012-8252(76)90052-0.
[46] M. Okrusch, S. Matthes, Mineralogie, Springer Berlin Heidelberg, Berlin, Heidelberg, 2014.
[47] S. Stopic, et al., Synthesis of magnesium carbonate via carbonation under high pressure in an autoclave, Metals 8 (2018) 993, https://doi.org/10.3390/met8120993.
[48] S. Stopic, et al., Synthesis of nanosilica via olivine mineral carbonation under high pressure in an autoclave, Metals 9 (2019) 708, https://doi.org/10.3390/met9060708.
[49] K. Baris, A. Ozarslan, N. Sahin, The assesment for CO 2 sequestration potential by magnesium silicate minerals in Turkey. Cases of orhaneli-bursa and divrigi-sivas regions, Energy Explor. Exploit. 26 (2008) 293–309, https://doi.org/10.1260/014459808787945362.
[50] Huijgen, W. Carbon dioxide sequestration by mineral carbonation. Feasibility of enhanced natural weathering as a CO2 emission reduction technology (s.n.], [S.l., 2007).
[51] M.H. Carr, R.S. Saunders, R.G. Strom, D.E. Wilhelms, The Geology of the Terrestrial Planets, U S Govt. Printing Office, Washington, DC, 1984.
[52] A. Lazaro, H. Brouwers, G. Quercia, J.W. Geus, The properties of amorphous nano-silica synthesized by the dissolution of olivine, Chem. Eng. J. 211–212 (2012) 112–121, https://doi.org/10.1016/j.cej.2012.09.042.
[53] N. Raza, et al., Synthesis and characterization of amorphous precipitated silica from alkaline dissolution of olivine, RSC Adv. 8 (2018) 32651–32658, https://doi.org/10.1039/C8RA06257A.
[54] C.B. Carter, M.G. Norton, Ceramic Materials. Science and Engineering, Springer Science+Business Media, LLC, New York, 2007, p. 106.
[55] A. Kaiser, M. Lobert, R. Telle, Thermal stability of zircon (ZrSiO4), J. Eur. Ceram. Soc. 28 (2008) 2199–2211, https://doi.org/10.1016/j.jeurceramsoc.2007.12.040.
[56] A. Spinthaki, G. Skordalou, A. Stathoulopoulou, K.D. Demadis, Modified macromolecules in the prevention of silica scale, Pure Appl. Chem. 88 (2016) 1037–1047, https://doi.org/10.1515/pac-2016-0807.
[57] C. Matus, et al., Mechanism of nickel, magnesium, and iron recovery from olivine bearing ore during leaching with hydrochloric acid including a carbonation pre-treatment, Metals 10 (2020) 811, https://doi.org/10.3390/met10060811.
[58] G.J. Stockmann, D. Wolff-Boenisch, N. Bovet, S.R. Gislason, E.H. Oelkers, The role of silicate surfaces on calcite precipitation kinetics, Geochim. Et. Cosmochim. Acta 135 (2014) 231–250, https://doi.org/10.1016/j.gca.2014.03.015.
[59] J.D. Rodriguez-Blanco, S. Shaw, L.G. Benning, The kinetics and mechanisms of amorphous calcium carbonate (ACC) crystallization to calcite, via vaterite, Nanoscale 3 (2011) 265–271, https://doi.org/10.1039/C0NR00589D.
[60] Q. Hu, et al., The thermodynamics of calcite nucleation at organic interfaces. Classical vs. non-classical pathways, Faraday Discuss. 159 (2012) 509, https://doi.org/10.1039/C2FD20124K.
[61] H.H. Teng, How ions and molecules organize to form crystals, Elements 9 (2013) 189–194, https://doi.org/10.2113/gselements.9.3.189.
[62] V.I. Kalikmanov, Nucleation Theory, Springer, Netherlands, Dordrecht, 2013.
[63] A. Fernandez-Martinez, Y. Hu, B. Lee, Y.-S. Jun, G.A. Waychunas, In situ determination of interfacial energies between heterogeneously nucleated CaCO3 and quartz substrates: thermodynamics of $CO_2$ mineral trapping, Environ. Sci. Technol. 47 (2013) 102–109, https://doi.org/10.1021/es3014826.
[64] J.J. de Yoreo, Principles of crystal nucleation and growth, Rev. Mineral. Geochem. 54 (2003) 57–93, https://doi.org/10.2113/0540057.
[65] M. Velbel, Bond Strength and the relative weathering rates om simple orthosilicatesORTHOSILICATES. Bond Strength and the relative weathering rates om simple orthosilicates, Am. J. Sci. 299 (1999) 679–696.
[66] R.L. Oliver, R.W. Nesbitt, D.M. Hausen, N. Franzen, Metamorphic olivine in ultramafic rocks from Western Australia, Contr. Mineral. Petrol. 36 (1972) 335–342, https://doi.org/10.1007/BF00444340.
[67] R.Y. Zhang, J.G. Liou, Exsolution lamellae in minerals from ultrahigh-pressure rocks, Int. Geol. Rev. 41 (1999) 981–993, https://doi.org/10.1080/00206819909465184.
[68] X. Liu, Z. Zhao, Y. Zhao, J. Chen, X. Liu, Pyroxene exsolution in mafic granulites from the Grove Mountains, East Antarctica: constraints on Pan-African metamorphic conditions, ejm 15 (2003) 55–65, https://doi.org/10.1127/0935-1221/2003/0015-0055.
[69] H. Ried, H. Fuess, Lamellar exsolution systems in clinopyroxene, Phys. Chem. Miner. 13 (1986) 113–118, https://doi.org/10.1007/BF00311901.
[70] L. Pittarello, et al., Two generations of exsolution lamellae in pyroxene from Asuka 09545: Clues to the thermal evolution of silicates in mesosiderite, Am. Mineral. 104 (2019) 1663–1672, https://doi.org/10.2138/am-2019-7001.
[71] S.-R. Zhao, G.-G. Zhang, H. Sun, R. Mason, X. He, Orientation of exsolution lamellae in mantle xenolith pyroxenes and implications for calculating exsolution pressures, Am. Mineral. 102 (2017) 2096–2105, https://doi.org/10.2138/am-2017-6009.
[72] D.B. van den Heuvel, E. Gunnlaugsson, L.G. Benning, Surface roughness affects early stages of silica scale formation more strongly than chemical and structural properties of the substrate, Geothermics 87 (2020), 101835, https://doi.org/10.1016/j.geothermics.2020.101835.
[73] A. Guha, Transport and deposition of particles in turbulent and laminar flow, Annu. Rev. Fluid Mech. 40 (2008) 311–341, https://doi.org/10.1146/annurev.fluid.40.111406.102220.
[74] L.G. Benning, G.A. Waychunas, Nucleation, growth, and aggregation of mineral phases: mechanisms and kinetic controls, in: S.L. Brantley, J.D. Kubicki, A.F. White (Eds.), Kinetics of Water-Rock Interaction, Springer, New York, NY, 2008, pp. 259–333.
[75] S. Song, Y. Cao, Textures and structures of metamorphic rocks. Encyclopedia of Geology, Elsevier, 2021, pp. 375–388.
[76] M.J. Wilson, Weathering of the primary rock-forming minerals: processes, products and rates, Clay Min. 39 (2004) 233–266, https://doi.org/10.1180/0009855043930133.